

Modeling and Control of Two Degree of Freedom Bionic Foot

Syed Salman Shah^{1*}, Muhammad Akif¹, Muhammad Arsalan¹, Syed Humayoon Shah², Taimoor Hassan¹, and Abid Imran¹.

¹Ghulam Ishaq Khan Institute of Engineering sciences and Technology, Faculty of Mechanical Engineering, Swabi, Topi, Pakistan

²Yuan Ze University, Department of Electrical Engineering, College of Electrical and communication Engineering, Taoyuan, Taiwan.

Abstract. Many people are affected by conditions like stroke, spinal cord diseases, cerebral palsy, and nerve injuries, leading to impaired leg function. Bionic foot assist in maintaining stability and posture, offering vital aid to those with mobility issues for improved quality of life and rehabilitation. Consequently, the use of bionic foot has increased. Bionic foot comprising electrical and mechanical components, provide comfort and support for individuals with mobility problems. An encouraging solution is to introduce bionic foot robots to help patients having mobility problems during their recovery journey. Designed to mimic the human skeletal system, these robots offer valuable assistance in restoring the natural gait cycle of patients having mobility problems. The proposed approach introduces a bionic foot designed to support movement of human ankle joint, marking a significant advancement in rehabilitation technology. Although human ankle joint actually exhibits 3 DOF motion, we consider 2 DOF motion of human ankle joint i.e., plantarflexion and dorsiflexion and, inversion and eversion as they are dominant during normal motion of human body. We designed two systems to control the motion of human ankle joint. Firstly, we have used two actuators, one for each degree of freedom to control the motion of ankle joint. Secondly, we have used an actuator to control the plantarflexion and dorsiflexion motion and Spring-Damper system to control the inversion and eversion motion of the human ankle joint. For both systems, we derive the mathematical model and then we design the PD controller using MATLAB/Simulink. For plantarflexion and dorsiflexion motion, we give standard pattern of human ankle gait as input and for inversion and eversion motion, we provide pulsating signal as our input for both the systems. After implementation, the response of the human ankle motion was precise, accurate and smooth. The torque applied by the actuators was also in the acceptable range.

1 INTRODUCTION

Bionic foot plays a vital role for impaired people to maintain their posture and stability. In the medical field, these wearables offer vital assistance to people with mobility problems, promoting the quality of their life and assisting in their rehabilitation. A large number of population is affected from stroke, spinal cord diseases, cerebral palsy, and nerve injury due to which their legs do not work properly [1], Hence the use of bionic foot and lower limb exoskeleton (LLE) is increased [2]. LLE is robot that can be worn for achieving comfort to people with mobility problems which consist of two part i.e. electrical part and mechanical part [3]. The mechanical part contains joints, links, springs and/or dampers etc. while the electrical part contains sensors, motors or other actuators and controllers [4], [5].

The ankle joint usually exhibits 3 degree of freedom motion i.e. plantarflexion and dorsiflexion, inversion and eversion and abduction and adduction. Each one has its own range of angles. The range of angles for various foot movements are as follows: $37.6^\circ \leq \text{angle} \leq 45.8^\circ$ for plantarflexion, $20.3^\circ \leq \text{angle} \leq 29.8^\circ$ for dorsiflexion, $14.5^\circ \leq \text{angle} \leq 22^\circ$ for inversion, $10^\circ \leq \text{angle} \leq 17^\circ$ for eversion, $15.4^\circ \leq \text{angle} \leq 25.9^\circ$ for abduction, and $22^\circ \leq \text{angle} \leq 36^\circ$ for adduction [6]. Dorsiflexion allows the foot to lift and avoid drag of foot with the ground. Foot drop is a condition in which the man cannot lift his foot and hence it drags on ground [7]. Similarly, other motions of the ankle joint also have their respective defects. Approximately 150,000 people is affecting from lower extremity amputations every year in united states [8] due to which they need LLE. It has been shown by the research that majority of the propulsion force is provided by the ankle joint during walking [9].

An ankle joint is the joint that bears most of the body weight unlike other joints of the body. If we put an actuator like motor on this joint, then it will experience maximum force [10], hence it is very essential to control the motion of ankle joint.

* Corresponding author: salman.mech4652@gmail.com

[2] investigates ANN algorithms for optimizing PID controller gains in a multi-joint Lower Limb Exoskeleton (LLE) for gait rehabilitation. Initially, PID parameters are tuned using the Ziegler-Nichols method based on the LLE's dynamic model. Various ANN-based algorithms are compared for tuning PID gains for each joint, resulting in improved performance and reduced overshoot values. This underscores the efficacy of ANN approaches in enhancing PID control for LLE systems in rehabilitation. [11], [12] used feedback linearization control of the exoskeleton robot, which converts the nonlinear system into the linear system which can be easily controlled using only PID tuning. [13] proposes an adaptive PID controller for a multi-joint lower extremity exoskeleton system, integrating metaheuristic algorithms with PID feedback. Using the particle swarm optimization (PSO) algorithm, the controller shows superior convergence and adaptability in diverse scenarios, indicating practical implementation potential. [13] introduces a hybrid GA and PSO method to optimize a PID controller for a four-degree-of-freedom lower limb exoskeleton. Using transfer functions from a pendulum model, each link is controlled in a closed-loop PID system. The hybrid algorithm minimizes error by transitioning from GA to PSO for parameter optimization. [14] introduces a 3-degree-of-freedom (3DOF) lower limb rehabilitation robot (LLRR) to aid stroke patients and ease physiotherapist workload. The LLRR features adjustable hip, knee, and ankle joints. A control-oriented model is validated through simulation and experiments, facilitating the design of an adaptive robust sub-controller to ensure joint tracking, and overcome uncertainties. [15] introduces a lower limb rehabilitation robot for mobility-impaired individuals, employing a passive control mode to simulate leg movement without muscle engagement. It establishes system dynamics equations and a mathematical model for an AC servo motor. A PID controller is designed using MATLAB/Simulink, demonstrating excellent trajectory tracking performance and mimicking human motion for passive rehabilitation [16] develops a dynamic model for human lower extremities and incorporates a realistic friction model for joint simulation. An adaptive control scheme with 31 parameters ensures accurate trajectory tracking, supported by stability analysis using the Lyapunov stability approach. [12], [17] uses the adaptive mechanism for grasping irregular objects, the proposed system can be implemented in the hybrid part of the bionic foot for regaining its initial state after disturbance torque applied on the bionic foot. [18] uses the adaptive control algorithm for controlling the motion and compliance behavior of the lower limb exoskeleton robot. [19]–[22] proposed the adaptive compliance controllers for different lower limb exoskeletons and grippers. Adaptive control methods, including a PIDNN controller, were applied to mitigate system uncertainty associated with cable-driven actuators. In this paper, we assume two degrees of freedom of ankle joint as these two motions are dominant and are necessary for the proper stability of the person having mobility problem. We are designing a PD controller for this purpose as it is a widely used controller worldwide.

2 DYNAMIC MODELING

There are two sections of the mathematical modelling for our system i.e. for the case where both degrees of freedom are controlled by actuators and second for the case when one degree of freedom is controlled by actuator and other is controlled by spring-damper system. Let's derive mathematical models for both cases.

2.1 2-DOF-ACTIVE SYSTEM

By considering two actuators models, where both the motions are actuated by the motors. Consider a bionic foot having mass m and 2-DOF motion of the ankle joint as shown in :Schematic of Ankle joint 1. The mathematical model for the case is developed using an energy-based approach called the Lagrangian approach.

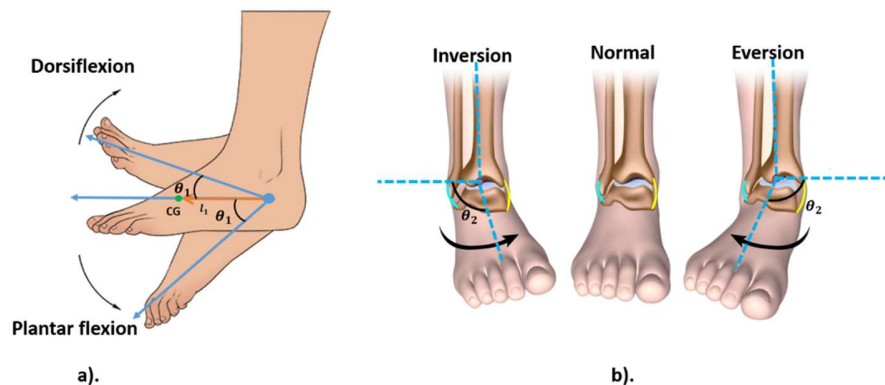


Figure 1: Schematic of Ankle joint. a). Dorsiflexion and Plantar flexion motion. b). Inversion and eversion motion [23]

Kinetic energy of the artificial foot can be found out by using the following formula [24]:

$$k = \frac{1}{2} m v_c^T v_c + \frac{1}{2} w^T I^c w \quad (1)$$

Where m is mass of bionic foot, v_c is the velocity vector, w is the angular velocity vector and I^c is moment of inertia matrix. The displacement and the velocity of the foot in x-direction are given by:

$$x_c = l_1 \cos \theta_1, \quad v_{x_c} = -l_1 \sin \dot{\theta}_1 \quad (2)$$

Where x_c and v_{x_c} are the displacement and velocity of bionic foot in x-direction respectively, l_1 is displacement between pivot point and the center of gravity and θ_1 denotes angle associated with plantarflexion and dorsiflexion. The displacement and velocity of the foot in y-direction are given by:

$$y_c = l_1 \sin \theta_1, \quad v_{y_c} = l_1 \cos \dot{\theta}_1 \quad (3)$$

Where y_c and v_{y_c} are the displacement and velocity of bionic foot in y-direction respectively. Now the velocity vector v_c of the bionic foot and its transpose are:

$$v_c = \begin{bmatrix} -l_1 \sin \dot{\theta}_1 \\ l_1 \cos \dot{\theta}_1 \end{bmatrix}, \quad v_c^T = [-l_1 \sin \dot{\theta}_1 \quad l_1 \cos \dot{\theta}_1] \quad (4)$$

$$v_c v_c^T = (l_1 \dot{\theta}_1)^2 \quad (5)$$

The angular velocity vector and the moment of inertia matrix are:

$$w = [\dot{\theta}_2 \quad 0 \quad \dot{\theta}_1], \quad I^c = \begin{bmatrix} I_{xx} & 0 & 0 \\ 0 & I_{yy} & 0 \\ 0 & 0 & I_{zz} \end{bmatrix} \quad (6)$$

Now we can find:

$$w^T I^c w = \dot{\theta}_2^2 I_{xx} + \dot{\theta}_1^2 I_{zz} \quad (7)$$

Now put equation (5) and (7) in equation (1):

$$k(\theta, \dot{\theta}) = \frac{1}{2} m l_1^2 \dot{\theta}_1^2 + \frac{1}{2} (\dot{\theta}_2^2 I_{xx} + \dot{\theta}_1^2 I_{zz}) \quad (8)$$

Now Potential energy u of the artificial foot can be found out by using the following formula:

$$u(\theta) = -m g_o^T P_c^o, \quad u(\theta) = -m \begin{bmatrix} 0 & -g & 0 \end{bmatrix} \begin{bmatrix} l_1 \cos \theta_1 \\ l_1 \sin \theta_1 \\ 0 \end{bmatrix} \quad (9)$$

Where g_o is the gravity vector and P_c is the position vector. Gravity, we assume is in negative y direction that's why $g_y = -g$:

$$u(\theta) = m l_1 g \sin \theta_1 \quad (10)$$

Now the torque τ acting on the joint is given by:

$$\tau = \begin{bmatrix} \tau_1 \\ \tau_2 \end{bmatrix} = \frac{d}{dt} \frac{\partial k}{\partial \dot{\theta}} - \frac{\partial k}{\partial \theta} + \frac{\partial u}{\partial \theta} \quad (11)$$

Where τ_1 is the torque associated with θ_1 and τ_2 is torque associated with θ_2 .

$$\tau = \begin{bmatrix} (m l_1^2 + I_{zz}) \ddot{\theta}_1 + m l_1 g \cos \theta_1 \\ I_{xx} \ddot{\theta}_2 \end{bmatrix} \quad (12)$$

Hence, we can write equations for torque of two angular motions separately as:

$$\tau_1 = (m l_1^2 + I_{zz}) \ddot{\theta}_1 + m l_1 g \cos \theta_1 \quad (13)$$

$$\tau_2 = I_{xx} \ddot{\theta}_2$$

The state space equation of the above model is:

$$\tau = M(\theta) \ddot{\theta} + V(\theta, \dot{\theta}) + G(\theta) \quad (14)$$

Where:

$$M(\theta) = \begin{bmatrix} m l_1^2 + I_{zz} & 0 \\ 0 & I_{xx} \end{bmatrix}, \quad \ddot{\theta} = \begin{bmatrix} \ddot{\theta}_1 \\ \ddot{\theta}_2 \end{bmatrix}, \quad V(\theta, \dot{\theta}) = \begin{bmatrix} 0 \\ 0 \end{bmatrix} \quad \text{and} \quad G(\theta) = \begin{bmatrix} m l_1 g \cos \theta_1 \\ 0 \end{bmatrix}$$

Re-arranging for $\ddot{\theta}_1$ and $\ddot{\theta}_2$:

$$\ddot{\theta}_1 = \frac{\tau_1}{ml_1^2 + I_{zz}} - \frac{mgl_1 \cos \theta_1}{ml_1^2 + I_{zz}} \quad (15)$$

$$\ddot{\theta}_2 = \frac{\tau_2}{I_{xx}} \quad (16)$$

2.2 2-DOF-HYBRID SYSTEM

In this case we have one actuator for controlling θ_1 , which is dorsiflexion and plantarflexion, and for controlling θ_2 , which is inversion and eversion, we have spring-damper system. For spring-damper system, there will be an input angle to our system i.e. θ_{in} in case of any disturbance. Let F_{k_1} , F_{k_2} , F_{b_1} and F_{b_2} are the restoring forces exerted by the two springs having stiffness k_1 and k_2 and the two dampers having damping coefficients b_1 and b_2 respectively then the schematic and the free body diagrams are shown in Figure 2.

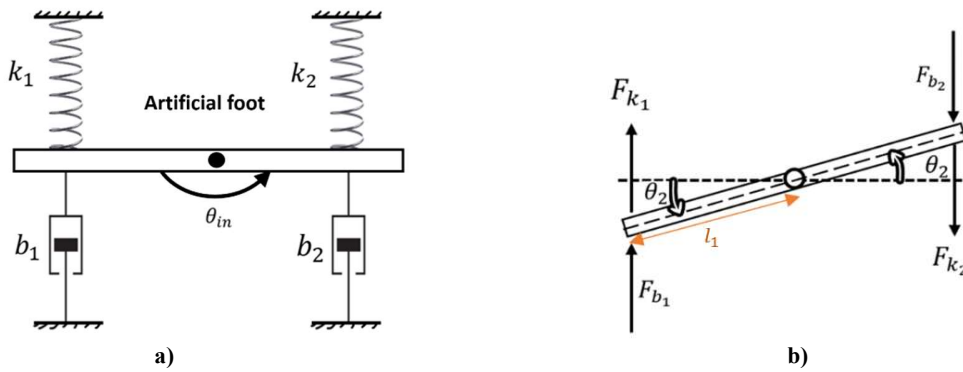


Figure 2: Spring-Damper system

Let $\theta_{in} > \theta_2$:

Applying Newton's second law:

$$\sum M = J\ddot{\theta}_2 \quad (17)$$

Where M denoted moment about pivot, J is the polar moment of inertia and θ_2 is angle associated with inversion and eversion.

$$F_{k_1}(l_2) \cos \theta_2 + F_{b_1}(l_2) \cos \theta_2 + F_{k_2}(l_2) \cos \theta_2 + F_{b_2}(l_2) \cos \theta_2 = J\ddot{\theta}_2 \quad (18)$$

If θ_2 is very small, then $\theta_2 \approx 0$ and $\cos \theta_2 \approx 1$. Here $J = I_{xx}$.

$$F_{k_1}(l_2) + F_{b_1}(l_2) + F_{k_2}(l_2) + F_{b_2}(l_2) = I_{xx}\ddot{\theta}_2 \quad (19)$$

Now let's find each force individually:

$$F_{k_1} = k_1 l_2 (\theta_{in} - \theta_2), F_{k_2} = k_2 l_2 (\theta_{in} - \theta_2), F_{b_1} = b_1 l_2 (\dot{\theta}_{in} - \dot{\theta}_2) \text{ and } F_{b_2} = b_2 l_2 (\dot{\theta}_{in} - \dot{\theta}_2) \quad (20)$$

Put in equation (19):

$$I_{xx}\ddot{\theta}_2 + k_1 l_2^2 (\theta_2 - \theta_{in}) + b_1 l_2^2 (\dot{\theta}_2 - \dot{\theta}_{in}) + k_2 l_2^2 (\theta_2 - \theta_{in}) + b_2 l_2^2 (\dot{\theta}_2 - \dot{\theta}_{in}) = 0 \quad (21)$$

If we are installing two springs and dampers of same nature, then $k_1 = k_2 = k$ and $b_1 = b_2 = b$.

$$\ddot{\theta}_2 = \frac{2kl_2^2}{I_{xx}} (\theta_{in} - \theta_2) + \frac{2bl_2^2}{I_{xx}} (\dot{\theta}_{in} - \dot{\theta}_2) \quad (22)$$

For actuator to control θ_1 i.e. dorsiflexion and plantarflexion, the mathematical model is given below:

$$\ddot{\theta}_1 = \frac{\tau_1}{ml_1^2 + I_{zz}} - \frac{mgl_1 \cos \theta_1}{ml_1^2 + I_{zz}} \quad (23)$$

It is like that of the two actuators system.

3 PHYSICAL PARAMETERS

The mathematical model has been developed in terms of the physical parameters, so it is very important to define the physical parameters. The moment of inertia of the foot is found by assuming foot as link. In case of θ_2 , the axis of rotation passes through the center of mass, So:

$$I_{xx} = \frac{ml^2}{12} \quad (24)$$

Where $l = 2l_2$:

In case of θ_1 , the axis of rotation doesn't pass through the center of mass, So

$$I_{zz} = \frac{ml^2}{3} \quad (25)$$

The value of the stiffness of the spring is found by the formula:

$$k = \frac{d^4G}{64R^3N} \quad (26)$$

Where d is wire diameter, G is modulus of rigidity, R is the mean radius of the coil and N is number of turns of the spring. We assume the material of spring as stainless steel and appropriate values for d, R and N to find stiffness of our spring. For finding damping ratio, consider equation (21):

$$\ddot{\theta}_2 = \frac{2kl_2^2}{I_{xx}}(\theta_{in} - \theta_2) + \frac{2bl_2^2}{I_{xx}}(\dot{\theta}_{in} - \dot{\theta}_2) \quad (27)$$

Where $\theta_2 - \theta_{in} = e$. So:

$$\ddot{e} + \frac{2kl_2^2}{I_{xx}}(e) + \frac{2bl_2^2}{I_{xx}}(\dot{e}) = 0 \quad (28)$$

Comparing above equation with:

$$\ddot{e} + \omega_n^2(e) + 2\zeta\omega_n(\dot{e}) = 0 \quad (29)$$

$$\omega_n = \left(\frac{2kl_2^2}{I_{xx}}\right)^{\frac{1}{2}} \quad (30)$$

And:

$$\zeta = \frac{2bl_2^2}{2I_{xx}} \times \left(\frac{I_{xx}}{2kl_2^2}\right)^{\frac{1}{2}} \quad (31)$$

Our desired system is critically damped system. So, putting $\zeta = 1$ and solving for b:

$$b = \frac{\sqrt{2kl_{xx}}}{l_2} \quad (32)$$

After calculating the values, we have Table 1: Physical parameters.

Table 1: Physical parameters

Parameter	Notation	Values
Mass(foot)	m	1.2(kg)
Moment Arm for θ_1	l_1	0.1(m)
Moment Arm for θ_2	l_2	0.04(m)
Moment of Inertia for θ_1	I_{zz}	0.04(kgm ²)
Moment of Inertia for θ_2	I_{xx}	0.00064(kgm ²)
Gravitational Acceleration	g	9.8(ms ⁻²)
Stiffness	k	580(N/m)
Damping Coefficient	b	10.77(N×sec /m)

4 SIMULINK MODEL

In this section, the dynamic model is used in MATLAB/SIMULINK to apply the control techniques for both the systems, 2-DOF active, and 2-DOF active and passive, to evaluate the performance of our controller for the bionic foot.

4.1 2-DOF ACTIVE SYSTEM

Next, we proceed to simulate all the models in Simulink and observe their responses. Let's start by focusing on the two-actuators model. In Simulink, we've constructed a model specifically for dorsiflexion and plantarflexion movements. As per the mathematical model, the movements of dorsiflexion and plantarflexion, as well as inversion and eversion, are independent of each other, allowing us to address them separately. To simulate dorsiflexion and plantarflexion, we require a walking pattern as a reference. The human gait for ankle joint is shown in Figure 3. Normal person completes one gait cycle in 1.05s [25]. The gaits pattern involving four cycles is:

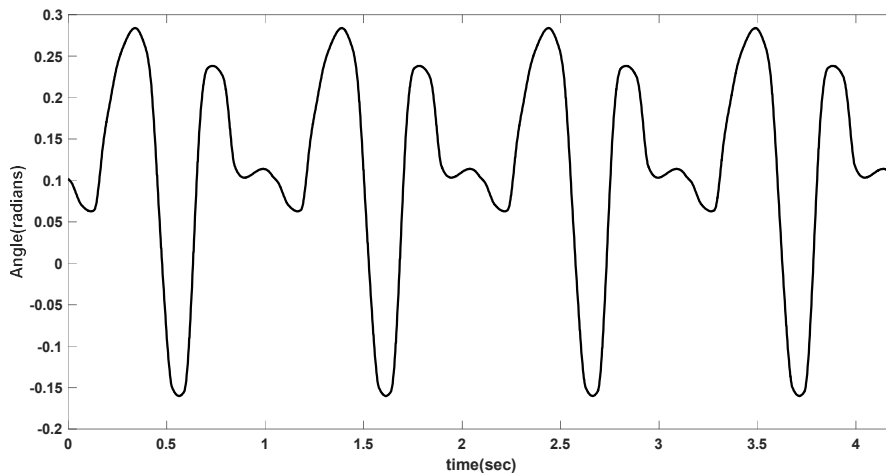


Figure 3: Ankle joint position vs Time [19].

It's crucial that the artificial foot's gait matches that of a natural foot for optimal function. Therefore, we incorporate a gait pattern resembling that of a properly functioning foot into our simulation. Our goal is to replicate this gait using our artificial foot and to avoid any disturbance responsible for inversion and eversion while considering torque limitations of the actuators. For the first and second actuator, putting in equation (15) and (16).

$$\ddot{\theta}_1 = \frac{\tau_1}{0.052} - 22.64 \cos \theta_1 \quad (33)$$

$$\ddot{\theta}_2 = 1562.5\tau_2 \quad (34)$$

We model these equations in Simulink by applying PD controllers as shown in Figure 4: Two actuators system flow diagram.

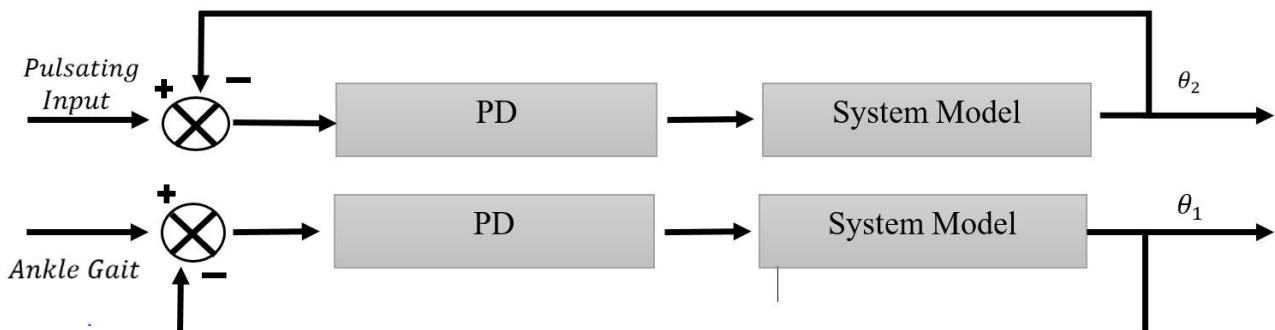


Figure 4: Two actuators system flow diagram

The torques in above models are adjusted by PD controllers and the values of the PD controller are $K_p=5000$ and $K_d=120$ for the first case and $K_p=200$ and $K_d=20$ for the second equation. These values of K_p and K_d have been found by the iterative process. First estimates were set by tuning using a built-in PD controller from Simulink and then for achieving the final desired values, the values were changed iteratively.

4.2 2-DOF-HYBRID SYSTEM

We must develop a closed loop system in which the dorsiflexion and the plantarflexion are controlled by the actuator and, the inversion and the eversion is controlled by the spring-damper system. The spring-damper system incorporates a spring and damper on each side of the pivot point. This setup is designed to counteract disturbances: when one spring compresses, the other extends, eliciting opposite reaction forces to restore equilibrium. While the springs bring the system to equilibrium, dampers are utilized to minimize oscillations around the mean position, ensuring stability and preventing unwanted foot oscillations. For dorsiflexion and plantarflexion and, eversion and inversion, the modelled equations are obtained by putting in equations (22) and (23).

$$\ddot{\theta}_2 = 2900(\theta_{in} - \theta_2) + 107.7(\dot{\theta}_{in} - \dot{\theta}_2) \quad (35)$$

$$\dot{\theta}_1 = \frac{\tau_1}{0.052} - 22.64 \cos \theta_1 \quad (36)$$

We model these equations in Simulink by applying PD controller to the first case. The torque in first model is adjusted by PD controller and the value of the PD controller are $K_p=5000$ and $K_d=120$ for the first case. The combine flow diagram is shown in Figure 5: Actuator and Spring-Damper system flow diagram.

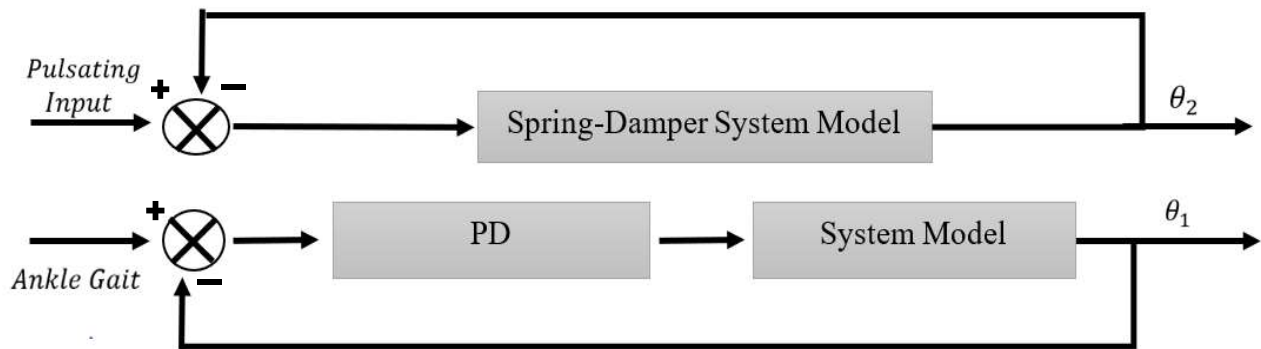


Figure 5: Actuator and Spring-Damper system flow diagram

5 RESULTS AND DISCUSSION:

In this section the results of all the simulations have been displayed. The graphs have been created by MATLAB and the simulations have been conducted in SIMULINK.

5.1 2-DOF ACTIVE SYSTEM

Initially, a simulation was performed employing two actuators. Subsequently, a PD controller was integrated into the system, and our modelled system captured the required response of human ankle gait. We plot the initial input human ankle gait and the output response for our system on single plot. The graph showing input and output angle responses across time is shown in Figure 6 (a). The simulation runs for a total of 4.2 seconds, with each gait cycle having a period of 1.05 seconds. Error is the difference between actual value of the response and the input value of the pattern at a particular value of time. The error graph as shown in Figure 6 (b) was also plotted over time, revealing that initially, the error is at its maximum value and it decreases with time. The error follows specific pattern because the plot of Figure 6 (a) is repeated after 1.05 seconds. Keeping in view the limitations of the motor, the torque was adjusted using the saturation block of Simulink to lie in the acceptable range of -3 to 3 Nm as shown in Figure 6 (c). In case of inversion and eversion motion of human ankle joint, an additional actuator was employed to address the disturbances. A pulsating input was introduced as a disturbance because the eversion and inversion motion mostly due to pulsating input while walking along the straight line, and the system's response was

recorded and plotted along with the input signal in Figure 6 (d). From Figure 6 (d), it is clear that the actuator reaches the input signal in approximately 0.3 seconds and when the person lifts the foot then in approximately 0.3 sec the foot comes to its initial state mean before putting the bionic foot on ground, the foot regains its initial state. A PD controller was utilized to mitigate disturbances by adjusting the torque, eliminating the need for an integral (I) controller due to the absence of steady-state error. Upon analyzing the input-output graph, we can study the system's error. These errors contain sudden jumps. This is due to the fact that whenever our input signal jumps from higher value to lower value or from lower value to higher value suddenly then our system takes some time i.e., 0.3sec to achieve the desired input. The graphical representation is shown in Figure 6(e). Since the model incorporates an actuator, it is imperative to assess the system's torque. Thus, the torque is graphically shown in Figure 6 (f), being in acceptable range of 3 to -3 Nm.

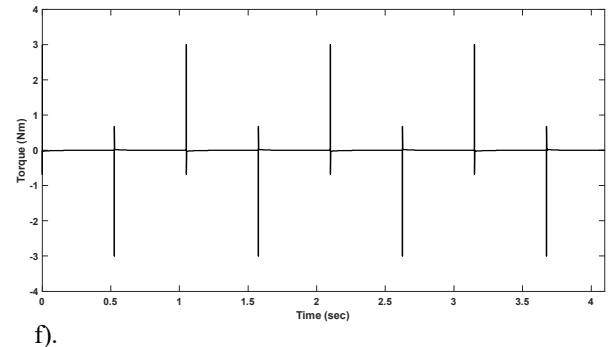
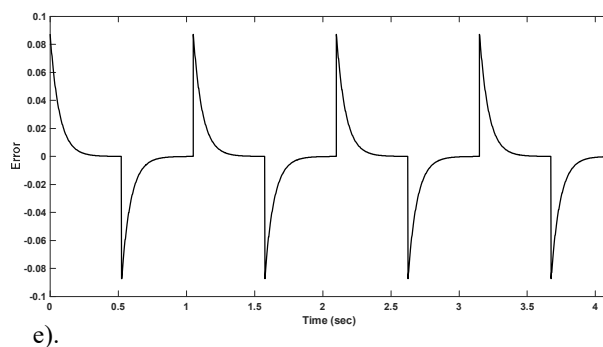
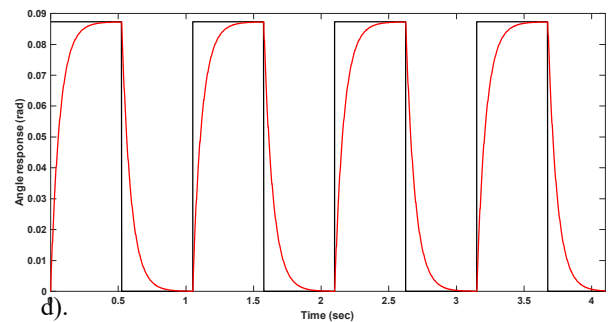
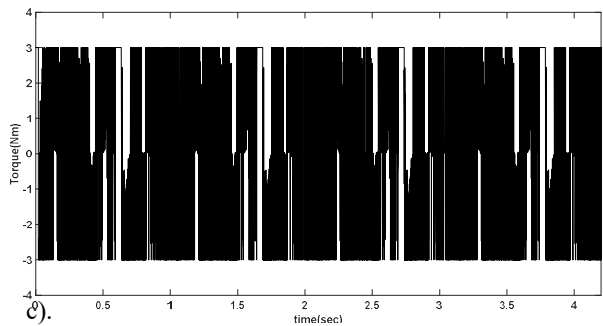
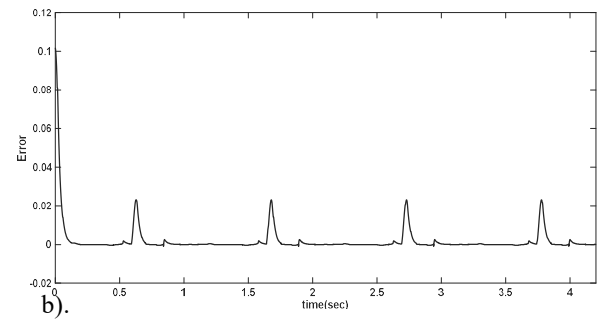
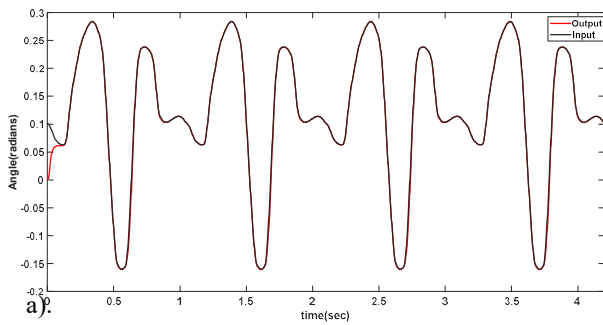
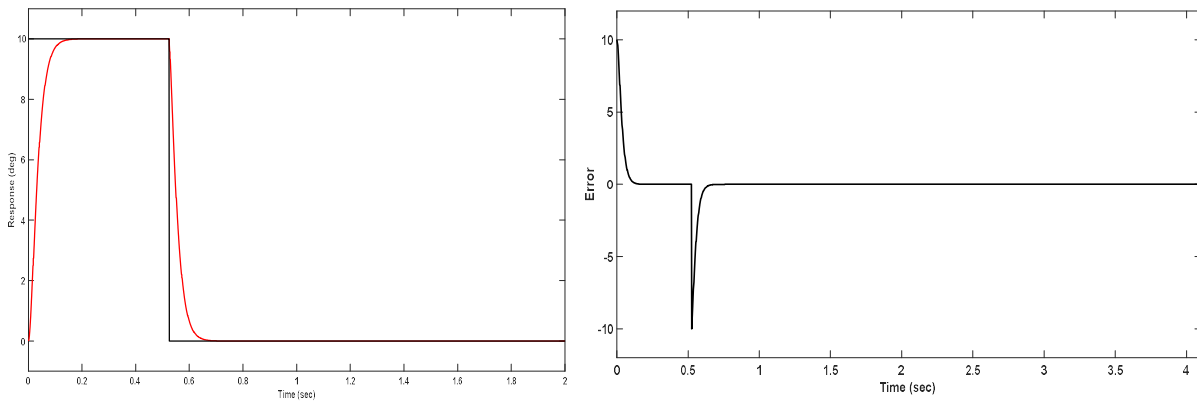


Figure 6: Simulation results of 2DOF active system, a). 1st actuator position vs time b). 1st actuator error vs time, c). 1st actuator torque vs time, d) 2nd actuator position vs time, e). 2nd actuator error vs time, f). 2nd actuator torque vs time

5.2 2-DOF HYBRID SYSTEM

In the integrated system, there exists no relation between the angles of dorsiflexion/plantarflexion and eversion/inversion. Consequently, the plots for dorsiflexion/plantarflexion remain identical for both the dual actuator and spring-damper configurations. The subsequent phase of the simulation involved implementing a controller for eversion and inversion, utilizing the spring-damper system within the model. This system responds to disturbances in the walking pattern by engaging to stabilize either in eversion or inversion. A pulse input was applied, and the resulting output response was observed and graphed for analysis, as depicted in Figure 7 (a). It is clear from Figure 7 (a) that in approximately 0.15 seconds, the bionic foot adopts the tilted position and similarly in same interval, the bionic foot regains its initial untitled position. Hence the foot base become parallel with ground before touching it. That why it is practice model. Plotting the input-output relationship allows us to visualize the system's error. It's evident from the graph that errors occur both at the start and end of the disturbance because our system takes some time to get stabilized. The error graph is displayed in Figure 7 (b).

The mathematical modeling of two separate models were developed and each system was then validated using MATLAB/SIMULINK. The results obtained from simulation showed that the hybrid system achieved better results as compared to the active system because for eversion and inversion the time required by hybrid system is almost half of the time required by two actuator system to reach the input pulsating signal or to regain itself before the foot touches the ground for the next step. The rise time in the hybrid system is fast as compared to the active system, which makes the system better and efficient.



a).

b).

Figure 7: simulation results of 2-DOF hybrid system, a). spring damper system joint angle vs time, b). spring damper system joint error vs time.

6. CONCLUSION

The bionic foot stands as a promising solution for individuals facing with mobility impairments, offering a pathway to stability and a restoration of their natural gait. Among the array of control strategies, the Proportional-Derivative (PD) controller emerges as a favorable choice for bionic legs due to its simplicity of implementation and rapid responsiveness, crucial for seamless interaction between the user and the device.

Simulation analyses underscore the efficacy of the PD controller in tracking reference trajectories, including the natural human gait patterns of ankle joint movements such as plantarflexion and dorsiflexion, as well as dynamic inputs like inversion and eversion. These findings reveal minimal tracking errors, indicating a robust alignment between the desired and actual movements. Furthermore, the torque exerted by the actuators remains within the prescribed range of -3 to 3Nm, ensuring safe and controlled motion. This improved performance has a great implication for the individual dependent on the bionic foot, providing a promising results in the restoring of gait cycle. This technology makes it easier for people to move around and do things on their own. It helps them feel more confident and independent in their everyday lives.

REFERENCES:

- [1] Y. J. Choo and M. C. Chang, "Commonly used types and recent development of ankle-foot orthosis: A narrative review," in *Healthcare*, 2021, p. 1046.
- [2] K. H. Al-Waeli, R. Ramli, S. M. Haris, Z. B. Zulkoffli, and M. S. Amiri, "Offline ANN-PID controller tuning on a multi-joints lower limb exoskeleton for gait rehabilitation," *IEEE Access*, vol. 9, pp. 107360–107374, 2021.
- [3] W. Huo, S. Mohammed, J. C. Moreno, and Y. Amirat, "Lower limb wearable robots for assistance and rehabilitation: A state of the art," *IEEE Syst. J.*, vol. 10, no. 3, pp. 1068–1081, 2014.
- [4] V. V. Kulkarni, V. A. Kulkarni, and R. Talele, "PID controller-based DC motor speed control," *Int. J. Recent Innov. Trends Comput. Commun.*, vol. 5, no. 9, pp. 35–38, 2017.
- [5] M. S. Amiri, R. Ramli, M. A. A. Tarmizi, M. F. Ibrahim, and K. Danesh Narooei, "Simulation and control of a six degree of freedom lower limb exoskeleton," *J. Kejuruter*, vol. 32, no. 2, pp. 197–204, 2020.
- [6] P. D. Phuoc, T. X. Tuy, and others, "Research control for ankle joint rehabilitation device," *J. Mech. Eng. Sci.*, vol. 16, no. 1, pp. 8743–8753, 2022.
- [7] D. P. Allen, R. Little, J. Laube, J. Warren, W. Voit, and R. D. Gregg, "Towards an ankle-foot orthosis powered by a dielectric elastomer actuator," *Mechatronics*, vol. 76, p. 102551, 2021.
- [8] T. R. Dillingham, L. E. Pezzin, and A. D. Shore, "Reamputation, mortality, and health care costs among persons with dysvascular lower-limb amputations," *Arch. Phys. Med. Rehabil.*, vol. 86, no. 3, pp. 480–486, 2005.
- [9] D. A. Winter, "Energy generation and absorption at the ankle and knee during fast, natural, and slow cadences.," *Clin. Orthop. Relat. Res.*, vol. 175, pp. 147–154, 1983.
- [10] T. Lee, I. Kim, and Y. S. Baek, "Design of a 2dof ankle exoskeleton with a polycentric structure and a bi-directional tendon-driven actuator controlled using a pid neural network," in *Actuators*, 2021, p. 9.
- [11] M. Moradnia, S. Pouladi, M. Aqib, and J.-H. Ryou, "Thermodynamic Analysis of Group-III-Nitride Alloying with Yttrium by Hybrid Chemical Vapor Deposition," *Nanomaterials*, vol. 12, no. 22, p. 4053, 2022.
- [12] M. Aqib *et al.*, "Design and implementation of shape-adaptive and multifunctional robotic gripper," *J. F. Robot.*, vol. 41, no. 1, pp. 162–178, 2024.
- [13] J. Liu, H. Fang, and J. Xu, "Online adaptive PID control for a multi-joint lower extremity exoskeleton system using improved particle swarm optimization," *Machines*, vol. 10, no. 1, p. 21, 2021.
- [14] J. Wu, J. Gao, R. Song, R. Li, Y. Li, and L. Jiang, "The design and control of a 3DOF lower limb rehabilitation robot," *Mechatronics*, vol. 33, pp. 13–22, 2016.
- [15] S. Gharatappeh, H. J. Asl, and J. Yoon, "Design of a novel Assist-As-Needed controller for gait rehabilitation using a cable-driven robot," in *2016 13th International Conference on Ubiquitous Robots and Ambient Intelligence (URAI)*, 2016, pp. 342–347.
- [16] S. K. Hasan and A. K. Dhingra, "An adaptive controller for human lower extremity exoskeleton robot," *Microsyst. Technol.*, vol. 27, no. 7, pp. 2829–2846, 2021.
- [17] M. Aqib, S. Pouladi, M. Moradnia, R. P. R. Kumar, N.-I. Kim, and J.-H. Ryou, "Strain accumulation and relaxation on crack formation in epitaxial AlN film on Si (111) substrate," *Appl. Phys. Lett.*, vol. 124, no. 4, 2024.
- [18] M. Arsalan, M. Tufail, S. G. Khan, and S. H. Shah, "Adaptive Learning Inertia Control of Lower Limb Exoskeleton Robot.," in *2021 International Conference on Robotics and Automation in Industry (ICRAI)*, 2021, pp. 1–6.
- [19] M. Arsalan, S. ur Rehman, M. Umair, A. Imran, and G. Iqbal, "Feedback Linearization Control of Lower Limb Exoskeleton Robot for Rehabilitation," in *MATEC Web of Conferences*, 2023, p. 1016.
- [20] S. H. Shah, M. Arsalan, S. G. Khan, M. T. Khan, and M. S. Alam, "Design and compliance control of a robotic gripper for orange harvesting," *Proc. - 22nd Int. Multitopic Conf. INMIC 2019*, pp. 1–5, 2019, doi: 10.1109/INMIC48123.2019.9022758.

- [21] S. H. Shah, M. S. Alam, M. Arsalan, I. ul Haq, S. G. Khan, and J. Iqbal, “Design and Adaptive Compliance Control of a Wearable Walk Assist Device,” in *2023 International Conference on Robotics and Automation in Industry (ICRAI)*, 2023, pp. 1–7.
- [22] S. Masroor, M. Arsalan, S. G. Khan, S. H. Shah, M. S. Alam, and A. Imran, “Design and Control of a Bionic Leg,” in *2023 International Multi-disciplinary Conference in Emerging Research Trends (IMCERT)*, 2023, pp. 1–6.
- [23] “<https://kinxlearning.com/blogs/news/ankle-joint-eversion-and-inversion>.”
- [24] M. W. Spong, J. De Schutter, H. Bruyninckx, and J. T.-Y. Wen, “Control of robots and manipulators,” in *Control System Applications*, CRC Press, 2018, pp. 165–193.
- [25] I. N. Afiah, H. Nakashima, and S. Muraki, “Age-related changes in walking motion of Japanese females: basic analysis of gait motion,” *대한인간공학회 학술대회논문집*, pp. 640–644, 2014.